Engineering Science and Technology, an International Journal 19 (2016) 1084–1098

HOSTED BY

Contents lists available at ScienceDirect

Engineering Science and Technology, an International Journal

journal homepage: http://www.elsevier.com/locate/jestch

Full Length Article

Multi-objective optimized fuzzy-PID controllers for fourth order nonlinear systems

M.J. Mahmoodabadi *, H. Jahanshahi

Department of Mechanical Engineering, Sirjan University of Technology, Sirjan, Iran

ARTICLE INFO

Article history:
Received 13 July 2015
Received in revised form
28 December 2015
Accepted 26 January 2016
Available online 27 February 2016

Keywords:
Fuzzy-PID controller
Multi-objective optimization
Genetic algorithm
Particle swarm optimization
Ball–beam system
Inverted pendulum system

ABSTRACT

In this paper, the Multi-objective Genetic Algorithm (MOGA) is used to obtain the Pareto frontiers of conflicting objective functions for the fuzzy-Proportional-Integral-Derivative (fuzzy-PID) controllers. The ball–beam and inverted pendulum fourth order nonlinear systems are regarded as nonlinear benchmarks. The considered objective functions for the ball–beam system are the distance error of the ball, the angle error of the beam, and the control effort. For the inverted pendulum system, the objective functions are the distance error of the cart, the angle error of the pendulum, and the control effort, which must be minimized simultaneously. The Pareto fronts are compared with those obtained by Multi-objective Particle Swarm Optimization (MOPSO). Four points are chosen from nondominated solutions of the obtained Pareto fronts based on the three conflicting objective functions and used for illustration of the state variables of the controlled systems. Obtained results elucidate the efficiency of the proposed controller in order to control nonlinear systems.

1. Introduction

Zadeh originally proposed the fuzzy logic and the fuzzy set theory [1,2]. Fuzzy systems are knowledge-based or rule-based systems formed via human knowledge and heuristics. They have been applied for a wide range of researching fields, such as control, communication, medicine, management, business, psychology, etc. The most significant applications and studies about fuzzy systems have concentrated on the control area [3–10]. The development of fuzzy-PID controllers for various engineering problems has been a major research activity in recent years. Duan et al. proposed an inherent saturation of the fuzzy-PID controller revealed due to the finite fuzzy rules [11]. Karasakal et al. applied fuzzy PID controllers based on an online tuning method and rule weighing in [12]. Boubertakh et al. proposed new auto-tuning fuzzy PD and PI controllers using reinforcement-learning algorithm for single-input single-output and two-input two-output systems [13]. In this way, the heuristic parameters of fuzzy-PID controllers have to be determined via an appropriate approach. A very effective way to choose these parameters is the use of evolutionary algorithms [14], such as the Genetic Algorithm (GA) [15] and particle swarm optimization (PSO) [16], etc. In [17], a constrained optimization of a simple fuzzy-PID system was designed for the online improvement of PID control performance during productive control runs. Oh et al. developed a design methodology for a fuzzy PD cascade controller for a ball–beam system using particle swarm optimization (PSO) [18]. Mahmoodabadi et al. designed fuzzy controllers for nonlinear systems using MOPSO based on the Lorenz dominance method [19]. Sahib proposed a type of controller consisting of proportional, integral, derivative, and second order derivative terms optimized using the PSO algorithm for an automatic voltage regulator system [20].

In this paper, a novel optimal fuzzy-PID control strategy is proposed and implemented on two nonlinear benchmark systems. Governing equations for ball–beam and inverted pendulum systems transformed to the state-space forms. Two fuzzy inference engines are utilized. Due to having some different objective functions, MOGA and MOPSO are applied and three and two dimensional Pareto front figures are shown. The conflicting objective functions for ball–beam system are the distance error of the ball, the angle error of the beam, and the control effort. For inverted pendulum system, those are the distance error of the cart, the angle error of the pendulum, and the control effort. The simulation results corresponding to the optimum points demonstrate that the designed controller has the superior performance in comparison with reported results in published literature.

The rest of this paper is organized as follows. Section 2 gives a brief description on the fuzzy-PID controller. Section 3 presents the multi-objective optimization genetic algorithm. In Section 4, the

* Corresponding author. Tel.: +98 34 423 36901; fax: +98 34 423 36900.
E-mail address: mahmoodabadi@sirjantech.ac.ir (M.J. Mahmoodabadi).
Peer review under responsibility of Karabuk University.

http://dx.doi.org/10.1016/j.jestch.2016.01.010
2215-0986/

dynamic models of the ball–beam and inverted pendulum systems are recalled. Furthermore, their optimal fuzzy-PID controllers, simulation results and comparison studies to verify the capability of the proposed controller are shown in this section. Finally, Section 5 concludes the paper.

2. Fuzzy-PID controller

The PID controller has a long history in the control engineering and is accepted in a lot of real applications due to the simple structure. Hence, this controller is widely used still in so many industrial applications despite offering several new techniques. Consider a fourth order nonlinear system with Equation (1).

$$\ddot{x} = f_1 + b_1 F$$

$$\ddot{\theta} = f_2 + b_2 F \tag{1}$$

where f_1, f_2, b_1, and b_2 are nonlinear functions and F is the control input. The state-space formulation of the system can be written as Equation (2).

$$\dot{x}_1 = x_2$$

$$\dot{x}_2 = x_3$$

$$\dot{x}_3 = f_1 + b_1 F \tag{2}$$

$$\dot{x}_4 = x_5$$

$$\dot{x}_5 = x_6$$

$$\dot{x}_6 = f_2 + b_2 F$$

where $x = [x_1, x_2, x_3, x_4, x_5, x_6] = \left[\int x, x, \dot{x}, \int \theta, \theta, \dot{\theta}\right]$ is the state vector with desired value $x^d = \left[x_1^d, x_2^d, x_3^d, x_4^d, x_5^d, x_6^d\right] = \left[\int x^d, x^d, \dot{x}^d, \int \theta^d, \theta^d, \dot{\theta}^d\right]$. The PID controller with inputs $e_x(t) = x - x^d$ and $e_\theta(t) = \theta - \theta^d$ and output $F_{pid}(t)$ is commonly defined as Equation (3).

$$\begin{aligned} F_{pid} = {} & K_{px} e_x(t) + K_{ix} \int_0^t e_x(\tau) d\tau + K_{dx} \frac{de_x(t)}{dt} \\ & + K_{p\theta} e_\theta(t) + K_{i\theta} \int_0^t e_\theta(\tau) d\tau + K_{d\theta} \frac{de_\theta(t)}{dt} \end{aligned} \tag{3}$$

where K_p, K_i, and K_d are the proportional, integral, and derivative gains, respectively. The adjustment and determination of these design parameters are key issues to design PID controllers. Hence, the fuzzy logic approach is applied to calculate the gains adaptively.

$$F_{Fuzzy\ pid} = \hat{K}_{ix} f_1 + \hat{K}_{px} f_2 + \hat{K}_{dx} f_3 + \hat{K}_{i\theta} f_4 + \hat{K}_{p\theta} f_5 + \hat{K}_{d\theta} f_6 \tag{4}$$

where $F_{Fuzzy\ pid}$ is the fuzzy-PID control action. $f_i, i = 1, 2, \ldots, 6$ are the fuzzy variables with inputs $\int x dt, x, \frac{dx}{dt}, \int \theta dt, \theta$ and $\frac{d\theta}{dt}$, respectively, and should be obtained by Single Input Fuzzy Inference Motor (SIFIM). Furthermore, in Equation (4), the variables $\hat{K}_{ix}$, $\hat{K}_{px}$, $\hat{K}_{dx}$, $\hat{K}_{i\theta}$, $\hat{K}_{p\theta}$ and $\hat{K}_{d\theta}$ are calculated by Equation (5).

$$\hat{K}_{ix} = K_{ix}^b + K_{ix}^r \Delta W_1$$

$$\hat{K}_{x} = K_{x}^b + K_{x}^r \Delta W_2$$

$$\hat{K}_{dx} = K_{dx}^b + K_{dx}^r \Delta W_3$$

$$\hat{K}_{i\theta} = K_{i\theta}^b + K_{i\theta}^r \Delta W_4$$

$$\hat{K}_{\theta} = K_{\theta}^b + K_{\theta}^r \Delta W_5$$

$$\hat{K}_{d\theta} = K_{d\theta}^b + K_{d\theta}^r \Delta W_6 \tag{5}$$

where $\Delta W_i, i = 1, 2, \ldots, 6$ are the fuzzy variables with inputs $\int x dt, x, \frac{dx}{dt}, \int \theta dt, \theta$ and $\frac{d\theta}{dt}$, respectively, and should be obtained by Preferrer Fuzzy Inference Motor (PFIM). K_{ix}^b, K_x^b, K_{dx}^b, $K_{i\theta}^b$, K_θ^b and $K_{d\theta}^b$ are the base variables and K_{ix}^r, K_x^r, K_{dx}^r, $K_{i\theta}^r$, K_θ^r and $K_{d\theta}^r$ are the regulation variables. The base and regulation variables can be obtained by the try and error process. However, one of the best solutions to find these to have an optimal controller is the use of optimization approaches such as evolutionary methods, such as the genetic algorithm.

3. Optimization

The genetic algorithm is an approach for solving optimization problems based on biological evolution via modification of a population of individual solutions, repeatedly. At each level, individuals are chosen randomly from the current population (as parents) then employed to produce the children for the next generation. In this paper, toolbox optimization of MATLAB (R2012a) with the following operators is implemented for optimal design of the fuzzy-PID controllers.

3.1. Population size

Increasing the population size enables the genetic algorithm to search more points and thereby obtain a better result. However, the larger the population size, the longer it takes for genetic algorithm to compute each generation.

3.2. Crossover options

Crossover options specify how the genetic algorithm combines two individuals, or parents, to form a crossover child for the next generation.

3.3. Crossover fraction

The crossover fraction specifies the fraction of each population, other than elite children, that is made up of crossover children.

3.4. Selection function

Selection options specify how the genetic algorithm chooses parents for the next generation.

3.5. Migration options

Migration options specify how individuals move between subpopulations. Migration occurs if you set population size to be a vector of length greater than 1. When migration occurs, the best individuals from one subpopulation replace the worst individuals in another subpopulation. Individuals that migrate from one subpopulation to another are copied. They are not removed from the source subpopulation.

3.6. Stopping criteria options

Stopping criteria determine what causes the algorithm to terminate.

In this paper, the configuration of the genetic algorithm is set as the values given in Table 1.

Furthermore, the multi-objective optimization of the proposed fuzzy-PID controller would be done with respect to twelve design variables and three objective functions. The base values [K_{ix}^b, K_{px}^b, K_{dx}^b, $K_{i\theta}^b$, $K_{p\theta}^b$, $K_{d\theta}^b$] and regulation values [K_{ix}^r, K_{px}^r, K_{dx}^r, $K_{i\theta}^r$, $K_{p\theta}^r$, $K_{d\theta}^r$] are

Table 1
Genetic algorithm configuration parameters.

Parameter	Value
Crossover fraction	0.8
Population size	200
Selection function	Tournament
Mutation function	Constraint-dependent
Crossover function	Intermediate
Migration direction	Forward
Migration fraction	0.2
Migration interval	20
Stopping criteria	Maximum generation 200

the design variables. For ball–beam system, the distance error of the ball, the angle error of the beam and the control effort, and for inverted pendulum system, the distance error of the cart, the angle error of the pendulum and the control effort, are the objective functions. In other words, for both systems, the objective functions can be written as Equations (6) to (8).

$$\text{Objective function } 1 = \int |x| dt \tag{6}$$

$$\text{Objective function } 2 = \int |\theta| dt \tag{7}$$

$$\text{Objective function } 3 = \int |F| dt \tag{8}$$

4. Optimal fuzzy-PID controller design

In this section, the optimal fuzzy-PID controller would be designed for the ball–beam and the inverted pendulum systems.

4.1. Ball–beam system

In the following, we consider the ball–beam system depicted in Fig. 1. The state vector is the system observable state vector $x = [x_1, x_2, x_3, x_4, x_5, x_6] = [\int x, x, \dot{x}, \int \theta, \theta, \dot{\theta}]$, including, respectively, the integral of the ball position, the ball position, the ball velocity, integral of the beam angle, the beam angle and the beam angular velocity. The dynamic equations of this system in the state-space form are expressed by Equation (9).

$$\dot{x}_1 = x_2$$

$$\dot{x}_2 = x_3$$

$$\dot{x}_3 = B\left[x_2 x_6^2 - g\sin(x_5)\right]$$

$$\dot{x}_4 = x_5$$

$$\dot{x}_5 = x_6$$

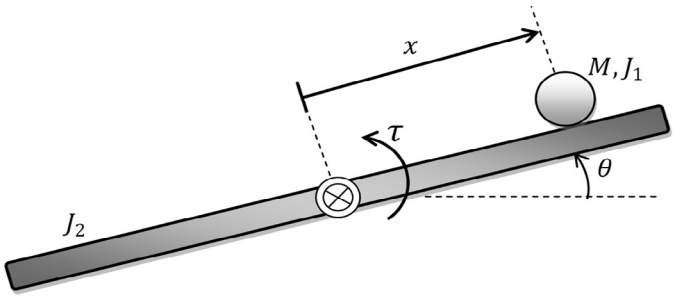

Fig. 1. Structure of the ball–beam system.

Table 2
State variables and the associated scaling factors and normalized forms for the ball–beam system.

Variable	Scaling factor	Normalized form
$\int x dt$	1	X_1
x	1	X_2
$\frac{dx}{dt}$	1	X_3
$\int \theta dt$	1	X_4
θ	45°	X_5
$\frac{d\theta}{dt}$	100°/s	X_6

$$\dot{x}_6 = \frac{\tau - 2Mx_2x_3x_6 - gMx_2\cos(x_5)}{J_1 + J_2 + Mx_2^2} \tag{9}$$

where M is the ball mass, g is the gravity acceleration, J_1 is the ball inertia moment, and J_2 is the beam inertia moment. The manipulated variable F is related with the torque τ by Equation (10).

$$\tau = 2Mx_2x_3x_6 + gMx_2\cos x_5 + \left(J_1 + J_2 + Mx_2^2\right)F \tag{10}$$

where F is the control input and $F = F_{Fuzzy\ pid}$. The system parameters used for simulation are $M = 0.05\ kg$, $J_1 = 2\times10^{-6}\ kgm^2$, $J_2 = 0.02\ kgm^2$, $g = 9.81\ \frac{m}{s^2}$, and $B = 0.7143$.

The initial and desired values are regarded as $x(0) = [x_1(0), x_2(0), x_3(0), x_4(0), x_5(0), x_6(0)] = [0, 0.5, 0, 0, -30°, 0]$ and $x^d = [x_1^d, x_2^d, x_3^d, x_4^d, x_5^d, x_6^d] = [0, 0, 0, 0, 0, 0]$, respectively.

The block diagram for the stabilization control of the ball–beam system shown in Fig. 2 illustrates that each of the state variables $\int x, x, v, \int \theta, \theta, \omega$ relevant to the ball–beam system is fed back and compared with its desired value. Since all of the desired values in the stabilization control are zeros, the variables are reversely inputted into the Norm block for normalization of the state variables by their scaling factors. The scaling factors and the normalized form of the outputs are given in Table 2.

For ball–beam system, the Single Input Fuzzy Inference Motor (SIFIM) has only one input, and for each normalized variable (Norm block output) an SIFIM is defined. Since there are 6 Norm block output items, 6 SIFIMs would be created. For each input item $X_i; i = 1, 2, \ldots, 6$, there is an SIFIM-i ($f_i; i = 1, 2, \ldots, 6$). The Preferrer Fuzzy Inference Motor (PFIM) represents the control priority order of each Norm block output. The PFIM blocks for $X_i; i = 1, 2, 3$ take the absolute values of the input items X_2 and X_5 as the antecedent variables, and the PFIM blocks for $X_i; i = 4, 5, 6$ take the absolute value of the input item X_5 as their antecedent variable. The membership functions of SIFIMs are shown in Table 3 and Fig. 3, and their rules are mentioned in Tables 4 and 5.

The output of $f_i, i = 1, 2, \ldots, 6$ for the ball and beam could be calculated using Equations (11) and (12).

Table 3
Membership functions of SIFIMs for the ball–beam system.

If	Then
$X_i \le -1$	$VB_i = 1$ $PO_i = 0$ $ZB_i = 0$
$-1 \le X_i \le 0$	$VB_i = -X_i$ $PO_i = X_i + 1$ $ZB_i = 0$
$0 \le X_i \le 1$	$VB_i = 0$ $PO_i = -X_i + 1$ $ZB_i = X_i$
$1 \le X_i$	$VB_i = 0$ $PO_i = 0$ $ZB_i = 1$

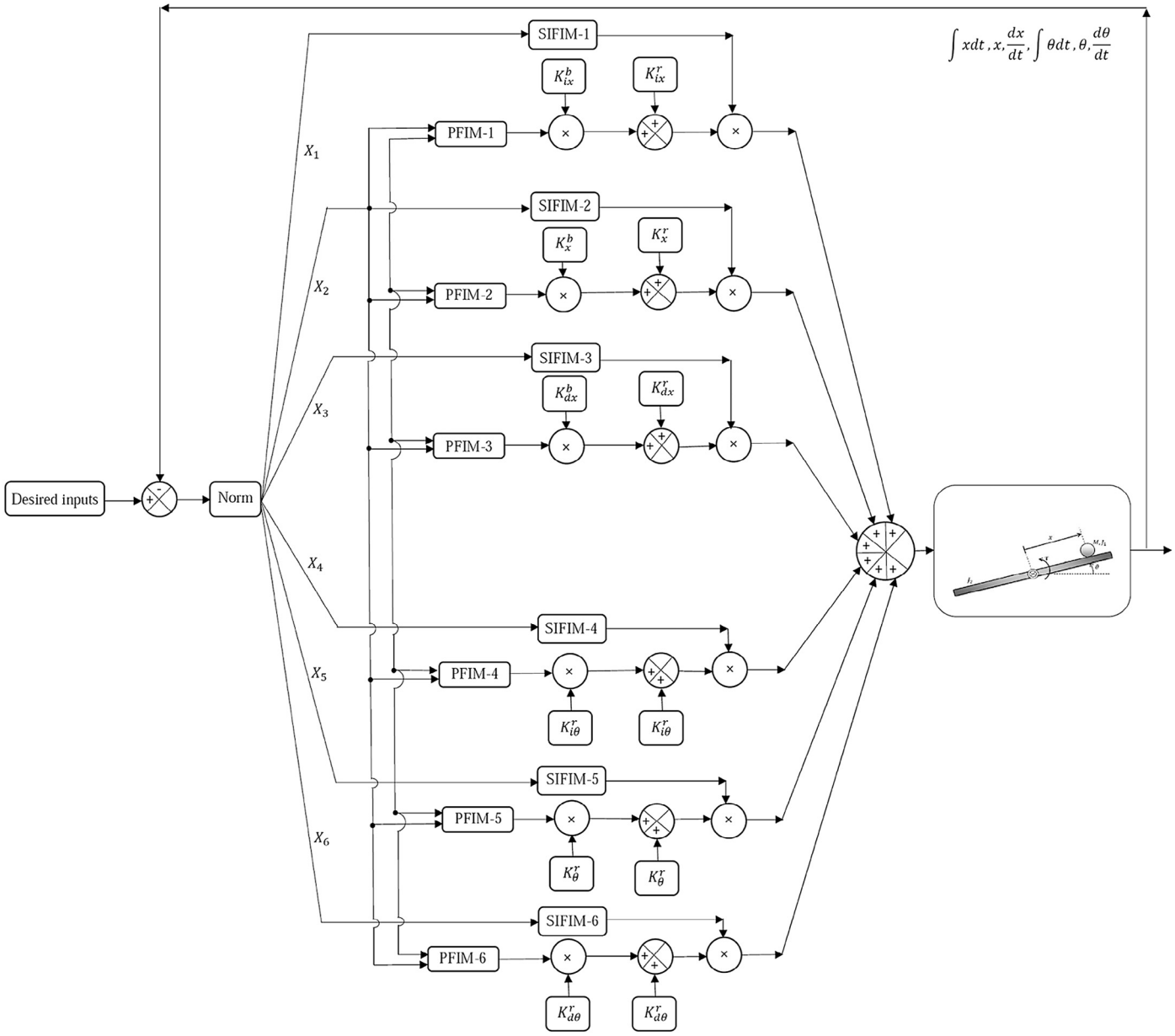

Fig. 2. The block diagram of fuzzy-PID control for the ball–beam system.

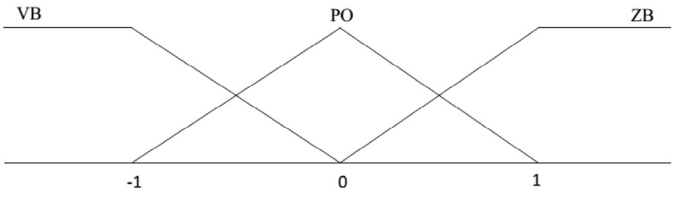

Fig. 3. Membership functions of SIFIMs for the ball–beam system.

$$f_i = \frac{VB_i \times \hat{f}_1 + PO_i \times \hat{f}_2 + ZB_i \times \hat{f}_3}{VB_i + PO_i + ZB_i} \quad i = 1, 2, 3 \tag{11}$$

$$f_i = \frac{VB_i \times \hat{f}_4 + PO_i \times \hat{f}_5 + ZB_i \times \hat{f}_6}{VB_i + PO_i + ZB_i} \quad i = 4, 5, 6 \tag{12}$$

where variables *VB*, *PO*, and *ZB* are given in Table 3 and Fig. 3. The membership functions of PFIMs are illustrated in Table 6 and Fig. 4, and their rules are shown in Tables 7 and 8.

Table 4
Fuzzy rules of SIFIMs for the ball.

If X_i $(i = 1, 2, 3)$	Then
VB_i	$\hat{f}_1 = -1$
PO_i	$\hat{f}_2 = 0$
ZB_i	$\hat{f}_3 = 1$

Table 5
Fuzzy rules of SIFIMs for the beam.

If X_i $(i = 4, 5, 6)$	Then
VB_i	$\hat{f}_4 = 1$
PO_i	$\hat{f}_5 = 0$
ZB_i	$\hat{f}_6 = -1$

Table 6
Membership functions of PFIM for the ball–beam system.

If	Then
$\|X_2\| \le 0.5$	$HS_1 = -2\|X_2\| + 1$
	$HM_1 = 2\|X_2\|$
	$HB_1 = 0$
$0.5 \le \|X_2\|$	$HS_1 = 0$
	$HM_1 = -2\|X_2\| + 2$
	$HB_1 = 2\|X_2\| - 1$
$\|X_5\| \le 0.5$	$HS_3 = -2\|X_5\| + 1$
	$HM_3 = -2\|X_5\|$
	$HB_3 = 0$
$0.5 \le \|X_5\|$	$HS_3 = 0$
	$HM_3 = -2\|X_5\| + 2$
	$HB_3 = 2\|X_5\| - 1$

The outputs of PFIMs for ball and beam, ΔW_1, ΔW_2, ΔW_3, ΔW_4, ΔW_5 and ΔW_6, can be calculated by Equations (13) and (14).

$$\Delta W_i = \frac{W_1 \times HS_1 \times HS_3 + W_2 \times HM_1 \times HS_3 + W_3 \times HB_1 \times HS_3 + W_4 \times HS_1 \times HM_3 + W5 \times HM_1 \times HM_3 + W_6 \times HB_1 \times HM_3}{HS_1 \times HS_3 + HM_1 \times HS_3 + HB_1 \times HS_3 + HS_1 \times HM_3 + HM_1 \times HM_3 + HB_1 \times HM_3 + HS_1 \times HB_3} \quad \ldots \frac{+W_7 \times HS_1 \times HB_3 + W_8 \times HM_1 \times HB_3 + W_9 \times HB_1 \times HB_3}{+HM_1 \times HB_3 + HB_1 \times HB_3}; \quad i = 1, 2, 3 \tag{13}$$

$$\Delta W_i = \frac{W_{10} \times HS_3 + W_{11} \times HM_3 + W_{12} \times HB_3}{HS_3 + HM_3 + HB_3}; \quad i = 4, 5, 6 \tag{14}$$

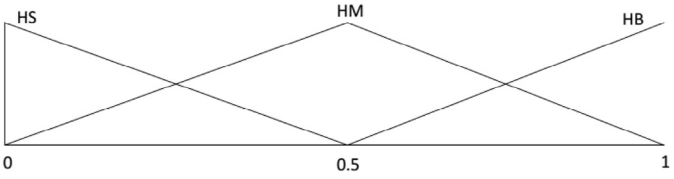

Fig. 4. Membership functions of PFIM for the ball–beam system.

Table 7
Rules of PFIMs for the ball.

If		Then
$\|X_2\|$	HS_1	$W_1 = 0$
$\|X_5\|$	HS_3	
$\|X_2\|$	HM_1	$W_2 = 0.5$
$\|X_5\|$	HS_3	
$\|X_2\|$	HB_1	$W_3 = 1$
$\|X_5\|$	HS_3	
$\|X_2\|$	HS_1	$W_4 = 0$
$\|X_5\|$	HM_3	
$\|X_2\|$	HM_1	$W_5 = 0$
$\|X_5\|$	HM_3	
$\|X_2\|$	HB_1	$W_6 = 0.5$
$\|X_5\|$	HM_3	
$\|X_2\|$	HS_1	$W_7 = 0$
$\|X_5\|$	HB_3	
$\|X_2\|$	HM_1	$W_8 = 0$
$\|X_5\|$	HB_3	
$\|X_2\|$	HB_1	$W_9 = 0$
$\|X_5\|$	HB_3	

Table 8
Fuzzy rules of PFIM for the beam.

If		Then
$\|X_5\|$	HS_3	$W_{10} = 0$
$\|X_5\|$	HM_3	$W_{11} = 0.5$
$\|X_5\|$	HB_3	$W_{12} = 1$

Table 9
Design variables of optimum point D for fuzzy-PID control of the ball–beam system.

Design variable	Value
K_{ix}^b	2.45
K_x^b	6.98
K_{dx}^b	7.75
$K_{i\theta}^b$	17.40
K_θ^b	32.09
$K_{d\theta}^b$	18.59
K_{ix}^r	1.24
K_x^r	7.07
K_{dx}^r	4.86
$K_{i\theta}^r$	5.79
K_θ^r	9.22
$K_{d\theta}^r$	8.71

After calculation of f_i and $\Delta W_i; i = 1, 2, \ldots, 6$, it is possible to define the fuzzy-PID controller via Equation (4).

In the following, the multi-objective optimization of the proposed fuzzy-PID controller would be done by MOGA and MOPSO [19] (with the same settings) with respect to the base and regulation parameters as design variables, and three objective functions as the distance error of the ball, the angle error of the beam and the control effort. The optimum points of the objective functions are illustrated in Figs. 5–8. Points A, B and C are the best points for objectives 1, 2 and 3, respectively, and point D is a trade-off point. The time responses of the ball position, beam angle and control input for these optimum points are depicted in Figs. 9–11.

Although the complete stabilization occurs and all the state variables converge to zero, by comparison of method proposed by Yi et al. [21] and this work, the superiority of this work from viewpoints of distance and angle error is obvious. In [21], as shown in Figs. 9 and 10, the ball position and beam angle reached the final state almost at 6 and 5.5 seconds, respectively, while this work can achieve almost 3 seconds for the ball position, 3.8 seconds for the beam angle and the maximum absolute of the control input is about 28.7 (point D). The values of design variables relative to point D and objective functions relative to points A, B, C, and D are given in Tables 9 and 10, respectively.

Table 10
Objective functions of points A, B, C, and D for fuzzy-PID control of the ball–beam system.

Point	Value
A	Objective function 1 = 1.79
	Objective function 2 = 38.13
	Objective function 3 = 6.98
B	Objective function 1 = 3.97
	Objective function 2 = 27.40
	Objective function 3 = 6.07
C	Objective function 1 = 2.47
	Objective function 2 = 32.65
	Objective function 3 = 4.41
D	Objective function 1 = 1.91
	Objective function 2 = 34.75
	Objective function 3 = 6.04

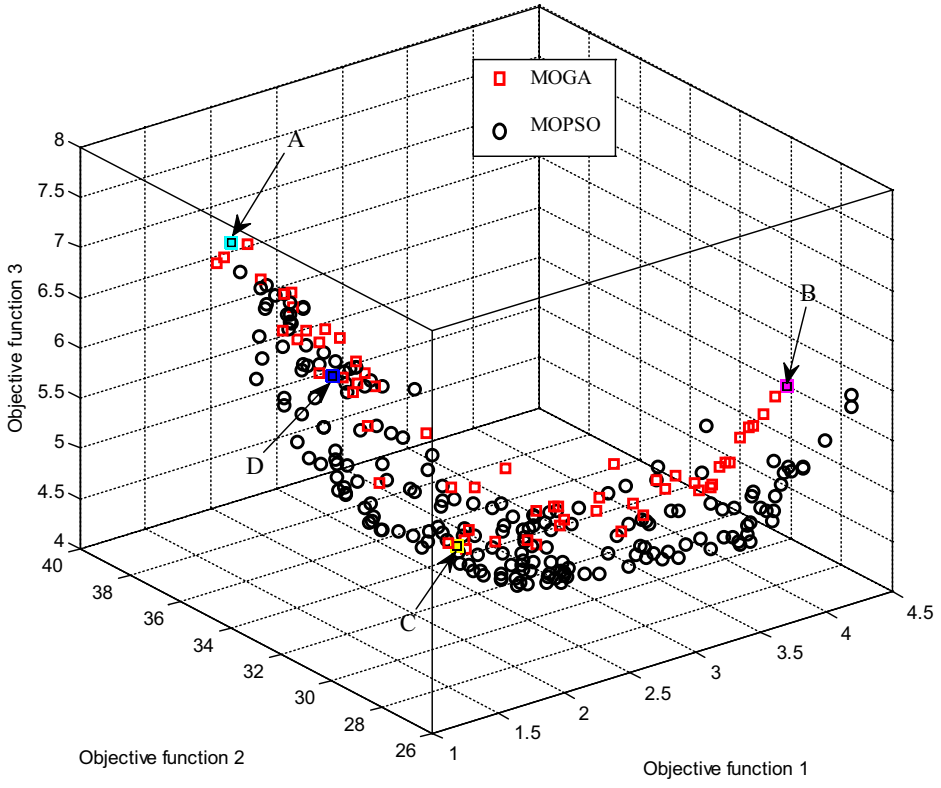

Fig. 5. Three-dimensional Pareto fronts of objective functions 1, 2 and 3 for the ball–beam system.

4.2. Inverted pendulum system

In the following, we consider the inverted pendulum system depicted in Fig. 12. $x=[x_1, x_2, x_3, x_4, x_5, x_6]=[\int x, x, \dot{x}, \int\theta, \theta, \dot{\theta}]$, including, respectively, integral of the cart position, the cart position, the cart velocity, integral of the pendulum angle, the pendulum angle and the pendulum angular velocity. The dynamic equations of this system in the state-space form are expressed by Equation (15).

$$\dot{x}_1 = x_2$$

$$\dot{x}_2 = x_3$$

$$\dot{x}_3 = \frac{\frac{4}{3}[F + m_p l_p x_6^2 \sin(x_5)] - m_p g sin(x_5)\cos(x_5)}{\frac{4}{3}(m_c + m_p) - m_p cos^2(x_5)}$$

$$\dot{x}_4 = x_5$$

$$\dot{x}_5 = x_6$$

$$\dot{x}_6 = \frac{(m_c + m_p) g sin(x_5) - [F + m_p l_p x_6^2 \sin(x_5)]\cos(x_5)}{\left[\frac{4}{3}(m_c + m_p) - m_p cos^2(x_5)\right] l_p} \quad (15)$$

where m_c is the mass of the cart, m_p is the mass of the pendulum, g is the gravity acceleration, and F is the control input and $F = 11 \times F_{Fuzzy\ pid}$. l_p is the length from the center of the pendulum to the pivot and equals to the half-length of the pendulum. For simulation, the following specifications are used $m_c = 1\,kg, m_p = 0.1\,kg, l_p = 0.5\,m, and\ g = 9.8\,\frac{m}{s^2}$.

The initial and desired conditions are $x(0) = [x_1(0), x_2(0), x_3(0), x_4(0), x_5(0), x_6(0)] = [0, 2, 0, 0, 0, 0]$ and $x^d = [x_1^d, x_2^d, x_3^d, x_4^d, x_5^d, x_6^d] = [0, 0, 0, 0, 0, 0]$, respectively. The block diagram for the stabilization control of the inverted pendulum system illustrated in Fig. 13 shows that each of the state variables $\int x, x, v, \int\theta, \theta, \omega$ relevant to inverted pendulum system is fed back and compared with its desired value. Since all of the desired values in the stabilization control are zero, the variables are directly inputted into the Norm block. The normalization of the state variables based on their scaling factors and creating input items $X_1, X_2, X_3, X_4, X_5, X_6$ from $\int x, x, v, \int\theta, \theta, \omega$, respectively, is done by the Norm block. The scaling factors and the normalized form of the Norm block outputs are given in Table 11.

Here, similar to fuzzy-PID control of the ball–beam system, two fuzzy inference engines SIFIM and PFIM are utilized. Each input item $X_i; i = 1, 2, \ldots, 6$ is guided to the SIFIM-i, and $f_i; i = 1, 2, \ldots, 6$ are its output corresponding to the input item X_i. PFIM represents the control priority order of each Norm block output. All of the PFIM blocks take the absolute value of the input item X_5 as their antecedent variable. The membership functions of SIFIMs are depicted in Table 12 and Fig. 14. The rules of the PFIMs are given in Tables 13 and 14.

Table 11
Scaling factors and normalized forms of the state variables for the inverted pendulum system.

Variable	Scaling factor	Normalized form
$\int x dt$	1	X_1
x	2.4 m	X_2
$\frac{dx}{dt}$	1	X_3
$\int\theta dt$	1	X_4
θ	30°	X_5
$\frac{d\theta}{dt}$	100°/s	X_6

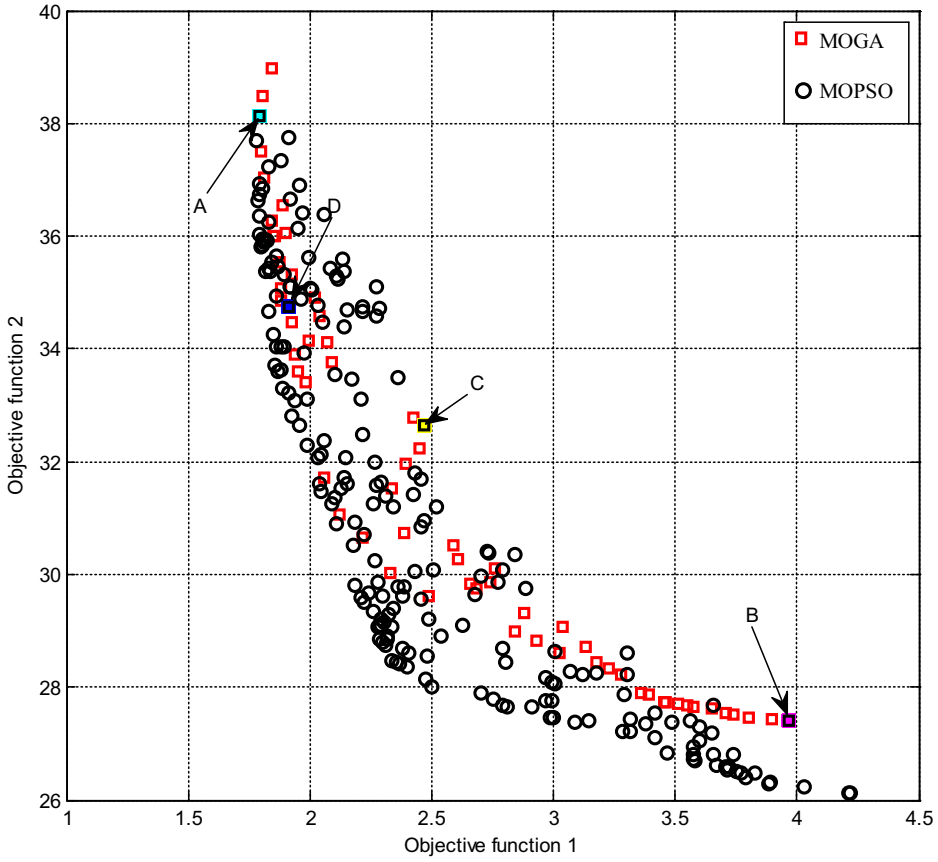

Fig. 6. Pareto fronts of objective functions 1 and 2 for the ball–beam system.

The output of SIFIM-i (f_i) for the cart and pendulum is calculated by Equations (16) and (17), respectively.

$$f_i = \frac{VB_i \times \hat{f}_1 + PO_i \times \hat{f}_2 + ZB_i \times \hat{f}_3}{VB_i + PO_i + ZB_i}; \quad i = 1, 2, 3 \tag{16}$$

Table 12
Membership functions of SIFIMs for the inverted pendulum system.

If	Then
$X_i \le -1$	$VB_i = 1$ $PO_i = 0$ $ZB_i = 0$
$-1 \le X_i \le 0$	$VB_i = -X_i$ $PO_i = X_i + 1$ $ZB_i = 0$
$0 \le X_i \le 1$	$VB_i = 0$ $PO_i = -X_i + 1$ $ZB_i = X_i$
$1 \le X_i$	$VB_i = 0$ $PO_i = 0$ $ZB_i = 1$

Table 13
Fuzzy rules of SIFIMs for the cart.

If X_i $(i = 1, 2, 3)$	Then
VB_i	$\hat{f}_1 = -1$
PO_i	$\hat{f}_2 = 0$
ZB_i	$\hat{f}_3 = 1$

$$f_i = \frac{VB_i \times \hat{f}_4 + PO_i \times \hat{f}_5 + ZB_i \times \hat{f}_6}{VB_i + PO_i + ZB_i}; \quad i = 4, 5, 6 \tag{17}$$

The membership functions of PFIMs are shown in Table 15 and Fig. 15. The rules of the PFIMs are given in Tables 16 and 17.

The outputs of PFIMs for ball and beam, ΔW_1, ΔW_2, ΔW_3, ΔW_4, ΔW_5 and ΔW_6, can be calculated by Equations (18) and (19).

$$\Delta W_i = \frac{W_1 \times HS_1 + W_2 \times HM_1 + W_3 \times HB_1}{HS_1 + HM_1 + HB_1}; \quad i = 1, 2, 3 \tag{18}$$

Table 14
Fuzzy rules of SIFIMs for the pendulum.

If X_i $(i = 1, 2, 3)$	Then
VB_i	$\hat{f}_4 = -1$
PO_i	$\hat{f}_5 = 0$
ZB_i	$\hat{f}_6 = 1$

Table 15
Membership functions of PFIM for inverted pendulum system.

If	Then
$\lvert X_2 \rvert \le 0.5$	$HS_1 = -2\lvert X_2 \rvert + 1$ $HM_1 = 2\lvert X_2 \rvert$ $HB_1 = 0$
$0.5 \le \lvert X_2 \rvert$	$HS_1 = 0$ $HM_1 = -2\lvert X_2 \rvert + 2$ $HB_1 = 2\lvert X_2 \rvert - 1$

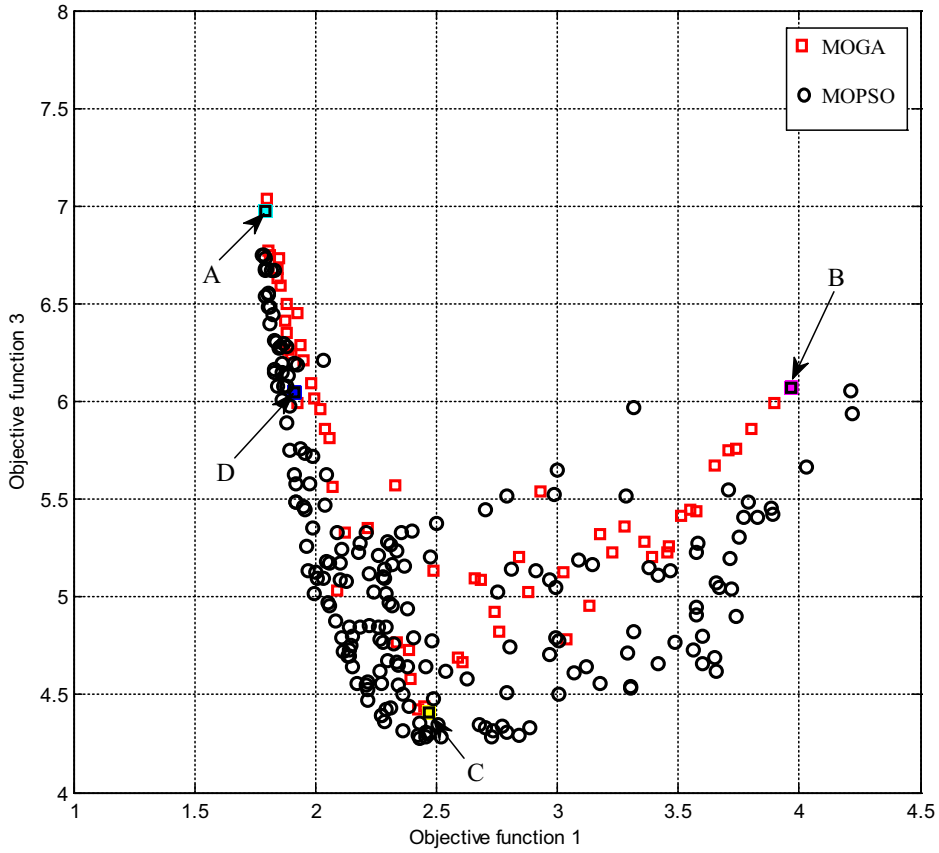

Fig. 7. Pareto fronts of objective functions 1 and 3 for the ball–beam system.

$$\Delta W_i = \frac{W_4 \times HS_1 + W_5 \times HM_1 + W_6 \times HB_1}{HS_1 + HM_1 + HB_1}; \quad i = 4, 5, 6 \tag{19}$$

where variables HS_1, HM_1, and HB_1 are given in Table 15 and Fig. 15.

After calculation of f_i and ΔW_i, it is possible to define the fuzzy-PID controller based on Equation (4).

The Pareto fronts obtained via the multi-objective genetic algorithm and particle swarm optimization [19] (with the similar configurations) are given in Figs. 16–19. Points A, B, and C are the best points of objectives 1, 2, and 3, respectively, and point D is selected as a trade-off optimum point. Trade-off is the best point that is obtained by substituting base variables and regulation variables of all the optimal points achieved of optimization via genetic algorithm and acquiring the best condition according to settling time and overshoot. The time responses of cart position, pendulum angular and derive force for the optimum points are illustrated in Figs. 20–22.

It is observable from Figs. 20–22 that all the state variables converge to zero and complete stabilization occurs. Moreover, the superiority of this work in comparison with proposed approach in [22] is obvious. In [22], the cart position and pendulum angle reached the final state almost in 7.2 and 7.5 seconds, respectively, while this work can achieve almost 3 seconds for the ball position and 4 seconds for the beam angle and the maximum absolute of the control input is about 8.02 (Point D). The values of design variables relative to point D and objective functions relative to points A, B, C, and D are given in Tables 18 and 19, respectively.

Table 16
Fuzzy rules of PFIMs for the cart.

If		Then
$\|X_5\|$	HS_1	$W_1 = 1$
$\|X_5\|$	HM_1	$W_2 = 0.5$
$\|X_5\|$	HB_1	$W_3 = 0$

Table 17
Fuzzy rules of PFIM for the beam.

If		Then
$\|X_5\|$	HS_1	$W_4 = 0$
$\|X_5\|$	HM_1	$W_5 = 0.5$
$\|X_5\|$	HB_1	$W_6 = 1$

Table 18
Design variables of optimum point D for fuzzy-PID control of the inverted pendulum system.

Design variable	Value
K_{ix}^b	0.029
K_x^b	0.583
K_{dx}^b	0.110
$K_{i\theta}^b$	2.88
K_θ^b	2.61
$K_{d\theta}^b$	1.92
K_{ix}^r	–0.030
K_x^r	0.291
K_{dx}^r	0.152
$K_{i\theta}^r$	3.79
K_θ^r	–1.50
$K_{d\theta}^r$	5.00

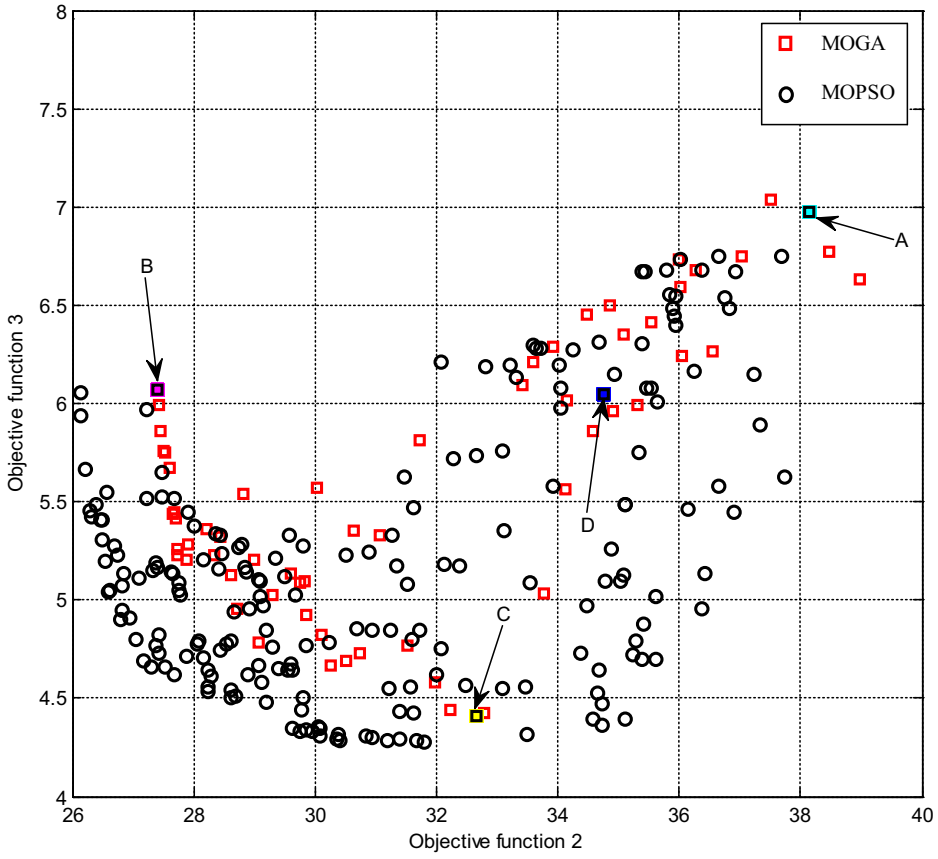

Fig. 8. Pareto fronts of objective functions 2 and 3 for the ball–beam system.

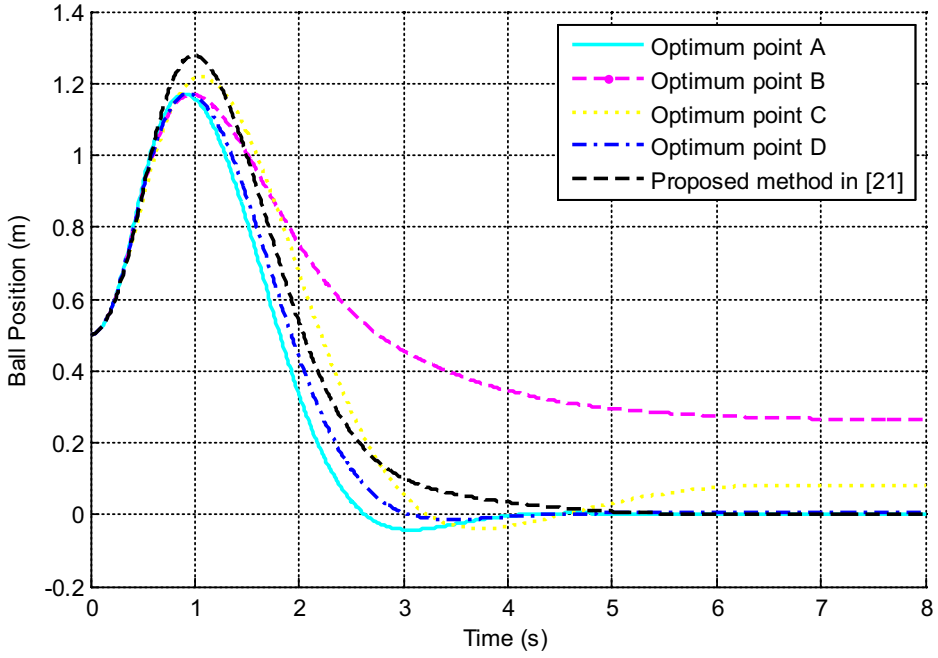

Fig. 9. Time response of the ball position for the ball–beam system.

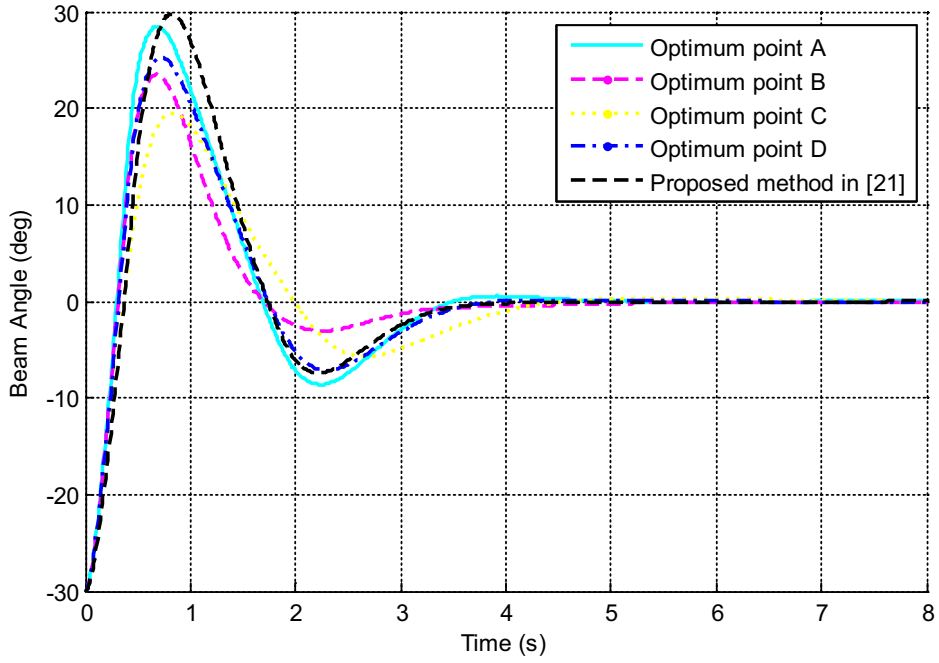

Fig. 10. Time response of the beam angle for the ball–beam system.

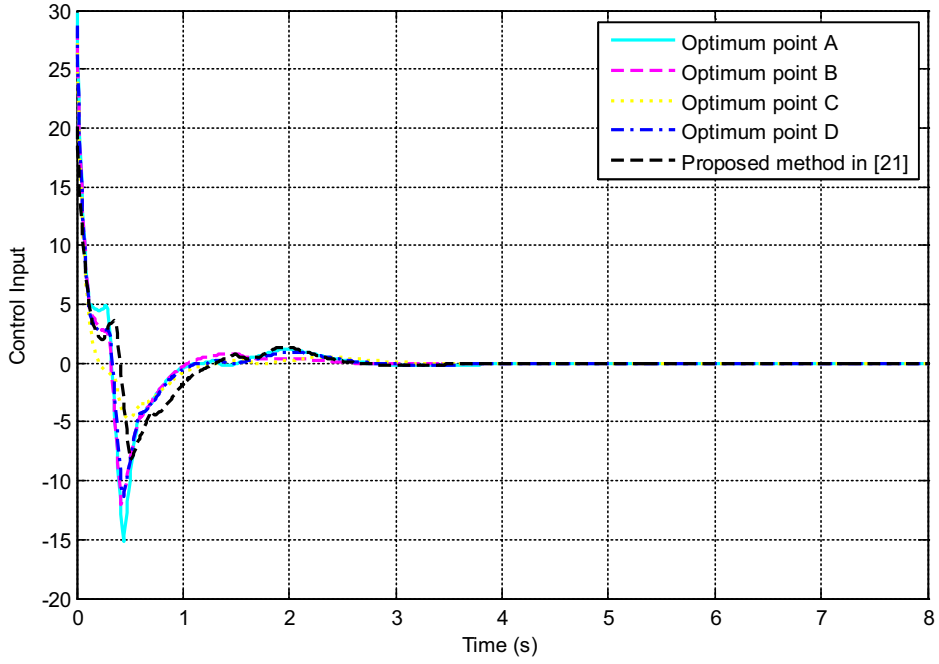

Fig. 11. Time response of the driving force for the ball–beam system.

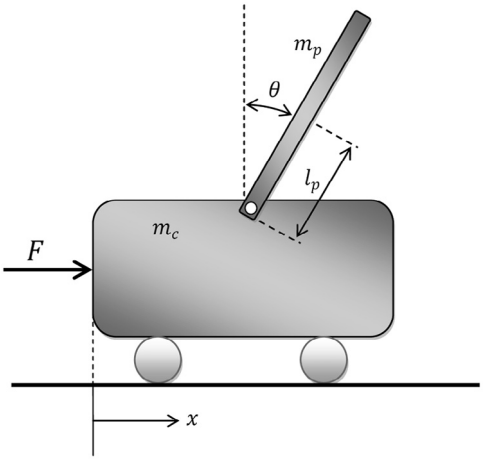

Fig. 12. Structure of the inverted pendulum system.

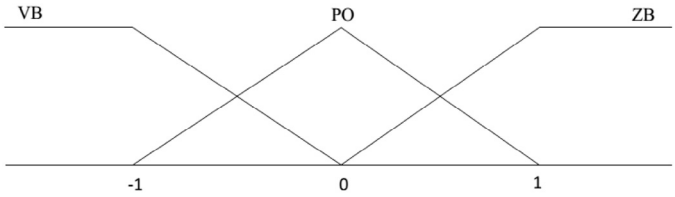

Fig. 14. Membership functions of SIFIMs for the inverted pendulum system.

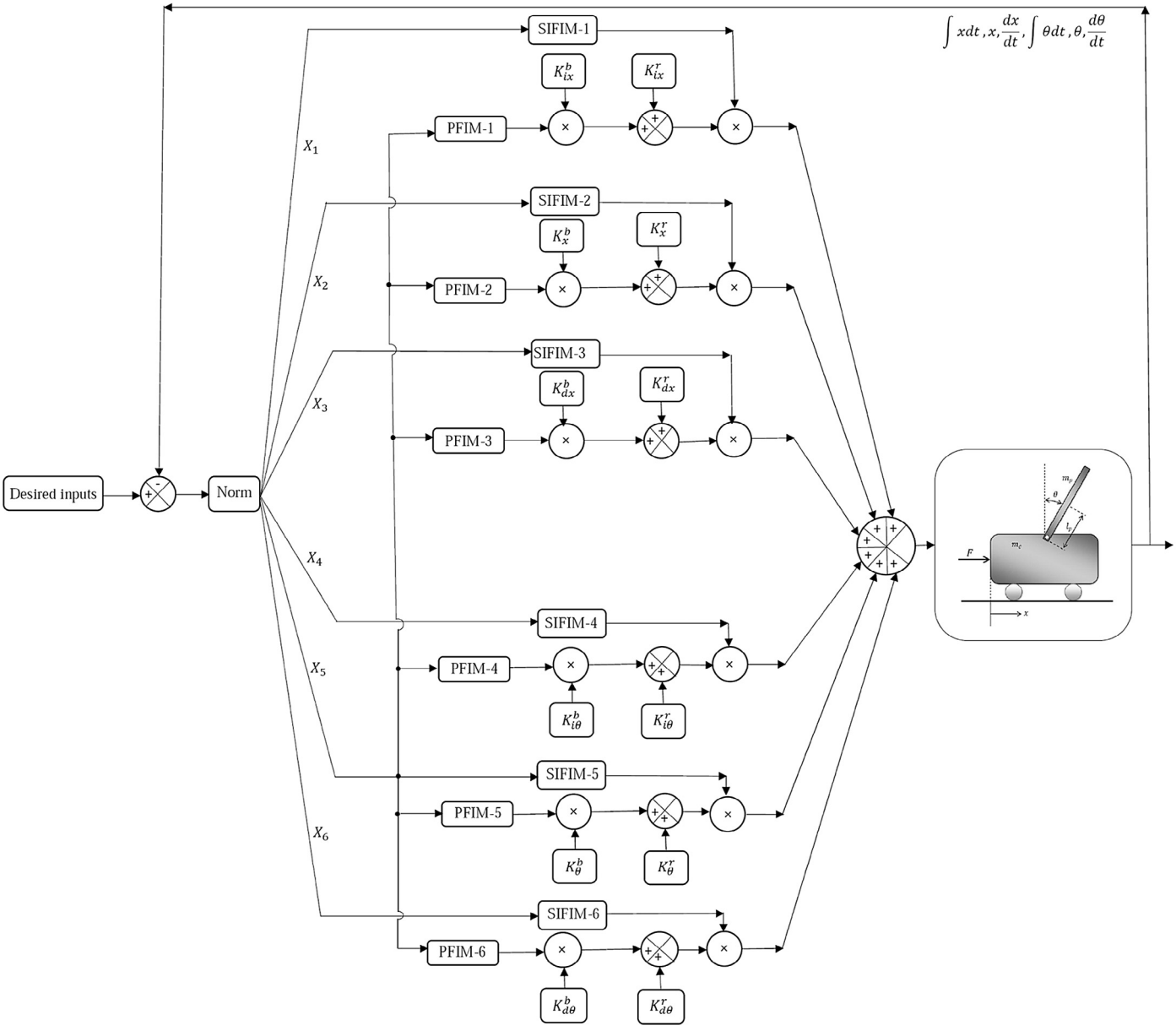

Fig. 13. Block diagram of fuzzy-PID control for the inverted pendulum system.

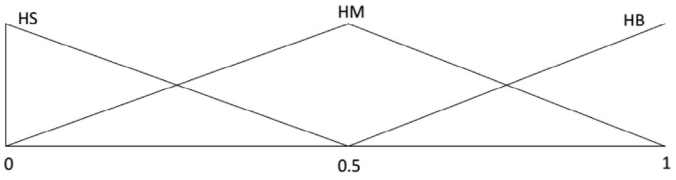

Fig. 15. Membership functions of PFIM for the inverted pendulum system.

5. Conclusion

In this work, multi-objective optimization algorithms, i.e. MOGA and MOPSO, were successfully used to optimum design the fuzzy-PID controllers for the ball–beam and inverted pendulum systems. An integral term was augmented to the state variables in order to eliminate the steady state errors and decrease the rising time. The conflicting objective functions for the ball–beam system were

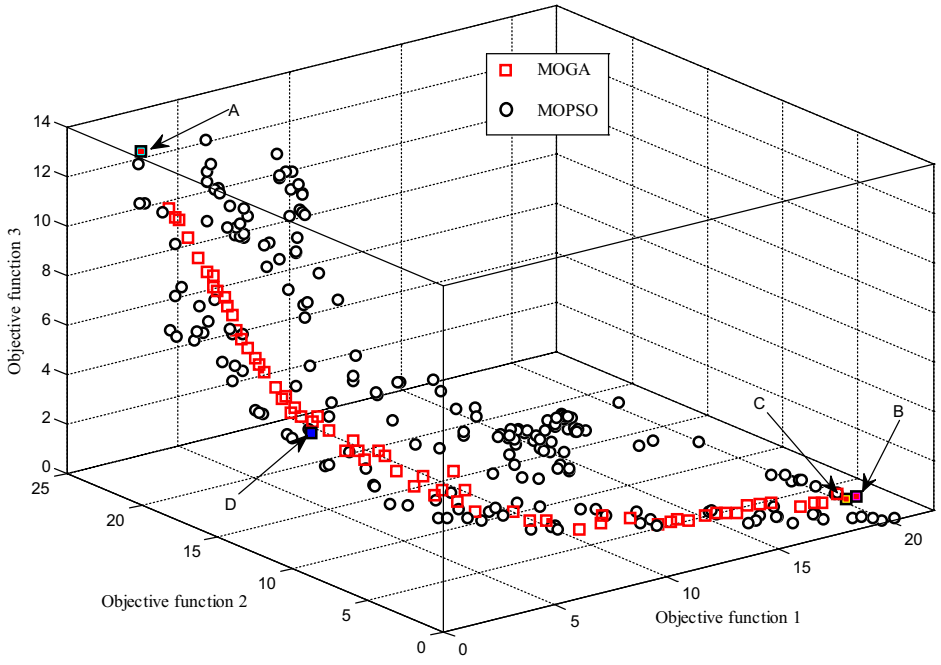

Fig. 16. Three-dimensional Pareto fronts of objective functions 1, 2 and 3 for the inverted pendulum system.

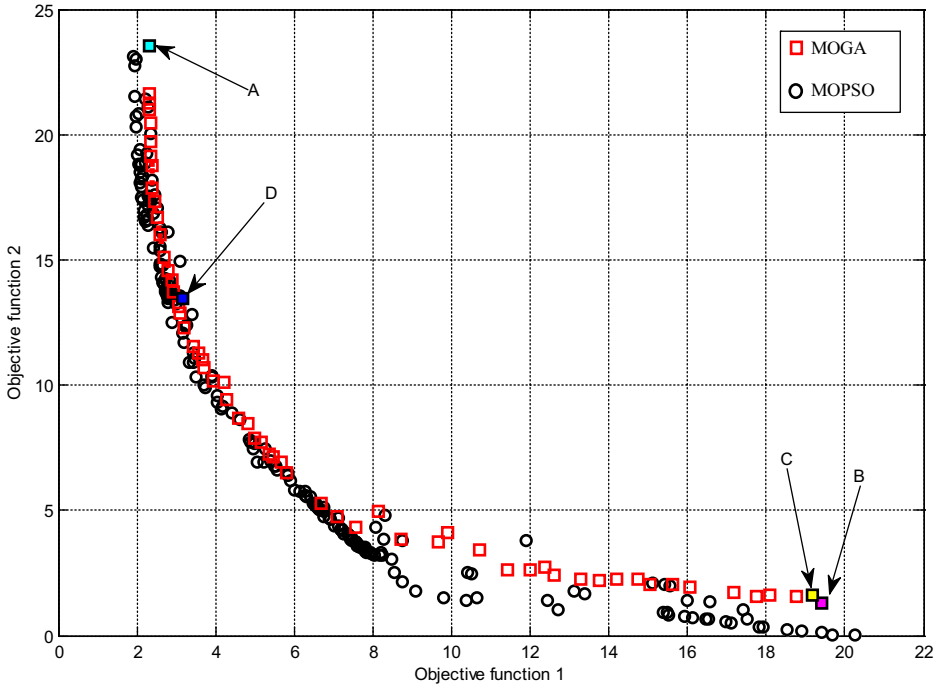

Fig. 17. Pareto fronts of objective functions 1 and 2 for the inverted pendulum system.

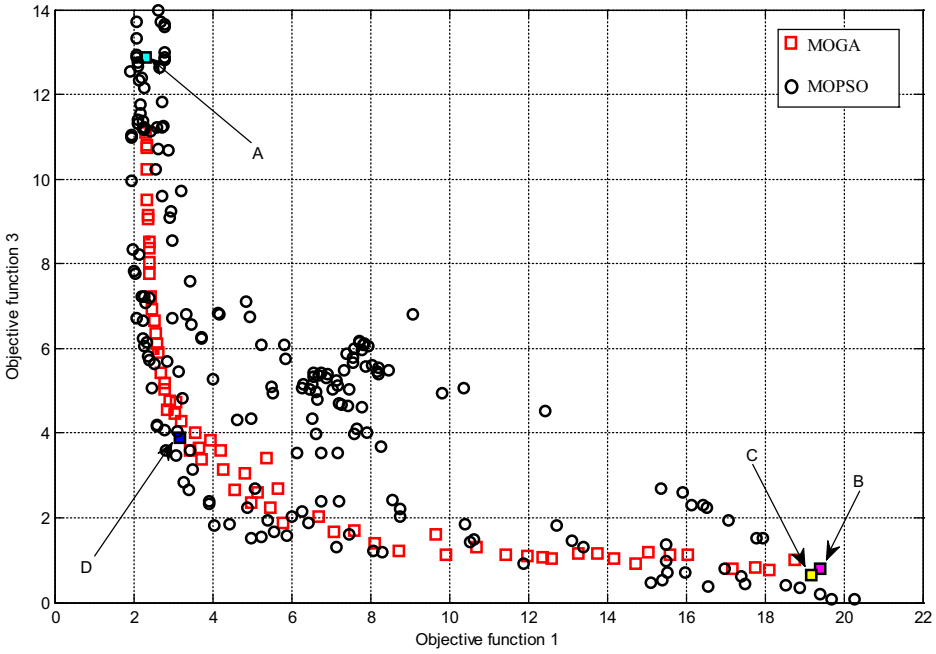

Fig. 18. Pareto fronts of objective functions 1 and 3 for the inverted pendulum system.

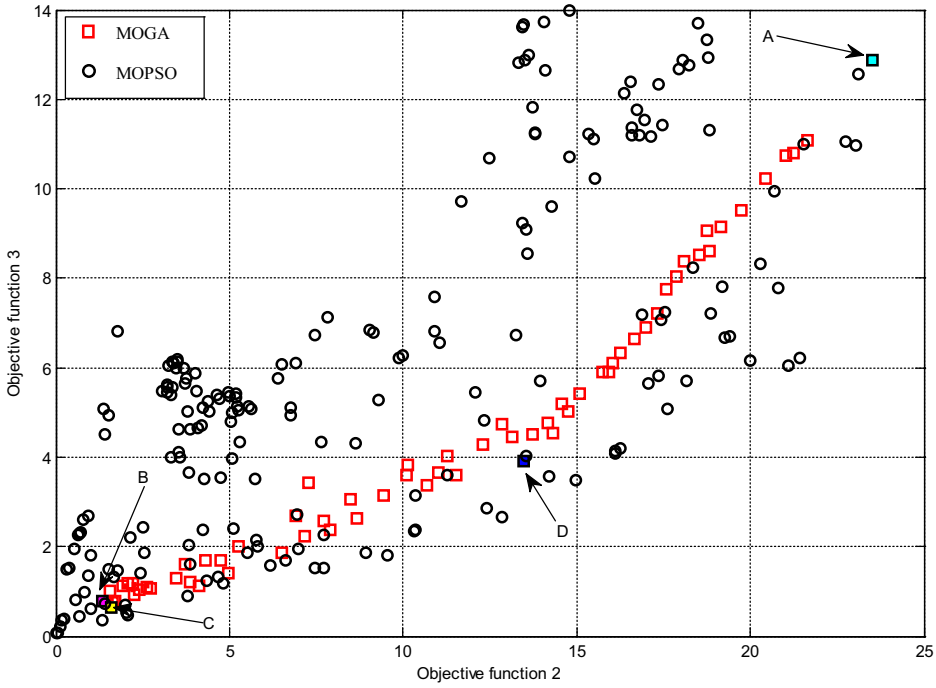

Fig. 19. Pareto fronts of objective functions 2 and 3 for the inverted pendulum system.

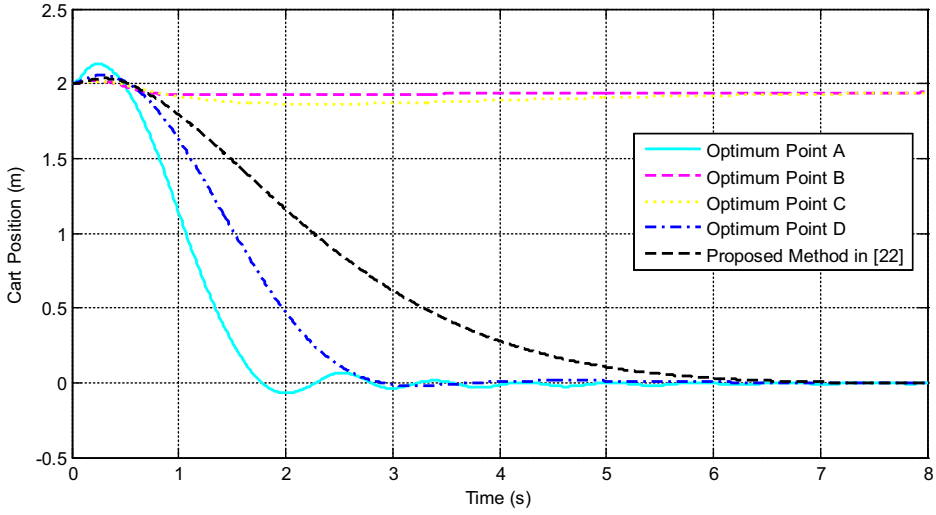

Fig. 20. Time response of the cart position for the inverted pendulum system.

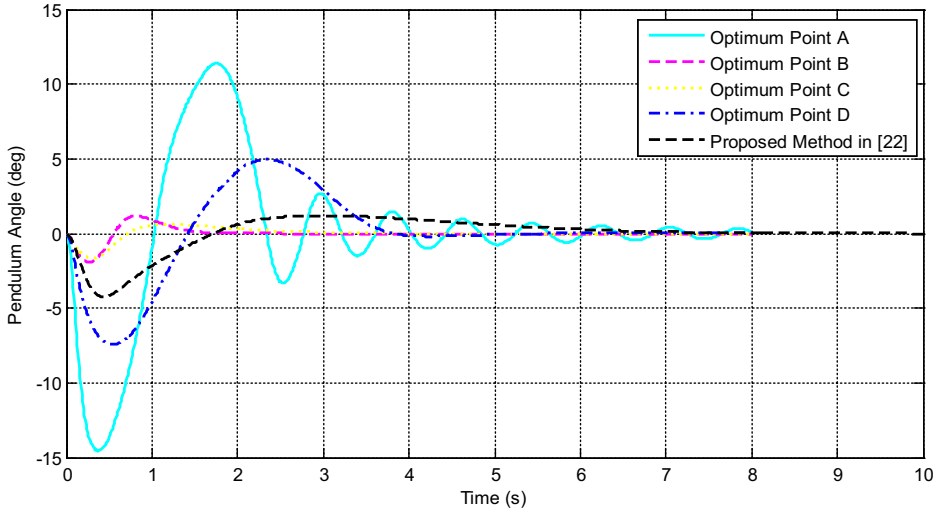

Fig. 21. Time response of the pendulum angle for the inverted pendulum system.

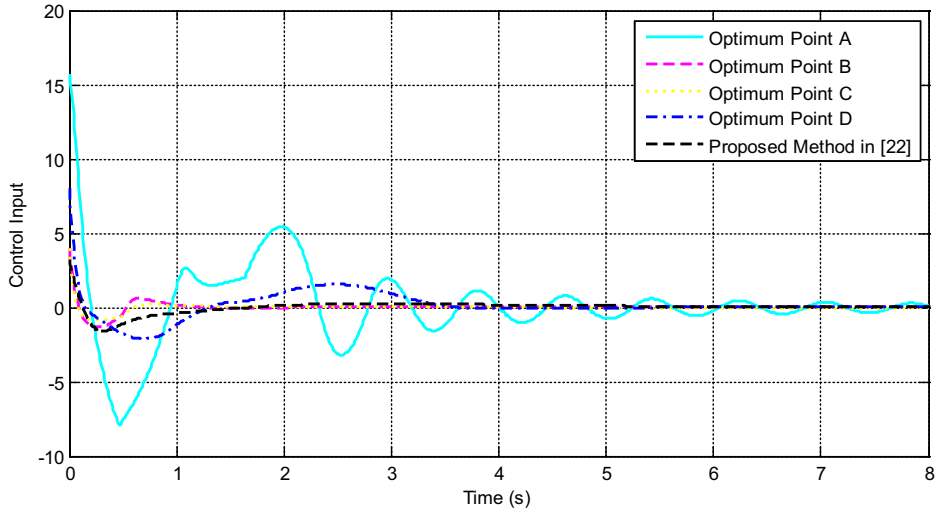

Fig. 22. Time response of the driving force for the inverted pendulum system.

Table 19
Objective functions of points A, B, C, and D for fuzzy-PID control of the inverted pendulum system.

Point	Value
A	Objective function 1 = 2.32 Objective function 2 = 23.52 Objective function 3 = 12.89
B	Objective function 1 = 19.41 Objective function 2 = 1.32 Objective function 3 = 0.79
C	Objective function 1 = 19.18 Objective function 2 = 1.60 Objective function 3 = 0.64
D	Objective function 1 = 3.18 Objective function 2 = 13.47 Objective function 3 = 3.90

considered as the distance error of the ball, the angle error of the beam, and the control effort. The conflicting objective functions for the inverted pendulum system were considered as the distance error of the cart, the angle error of the pendulum, and the control effort. The reported results demonstrated that the proposed methodology can effectively control the nonlinear systems.

References

[1] L.A. Zadeh, Fuzzy algorithms, Inform. Contr. 12 (1968) 94–102.
[2] L.A. Zadeh, Outline of a new approach to the analysis of complex systems and decision processes, IEEE Trans. Syst. Man Cybern. 3 (1) (1973) 28–44.
[3] H. Nasser, E.H. Kiefer-Kamal, H. Hu, S. Belouettar, E. Barkanov, Active vibration damping of composite structures using a nonlinear fuzzy controller, Compos. Struct. 94 (4) (2012) 1385–1390.
[4] P. Li, F.J. Jin, Adaptive fuzzy control for unknown nonlinear systems with perturbed dead-zone inputs, Acta Automat. Sinica 36 (4) (2010) 573–579.
[5] M. Marinaki, Y. Marinakis, G.E. Stavroulakis, Fuzzy control optimized by PSO for vibration suppression of beams, Control Eng. Pract. 18 (6) (2010) 618–629.
[6] D. Wang, X. Lin, Y. Zhang, Fuzzy logic control for a parallel hybrid hydraulic excavator using genetic algorithm, Automat. Constr. 20 (5) (2011) 581–587.
[7] R.E. Precup, M.B. Rădac, M.L. Tomescu, E.M. Petriu, S. Preitl, Stable and convergent iterative feedback tuning of fuzzy controllers for discrete-time SISO systems, Expert Syst. Appl. 40 (1) (2013) 188–199.
[8] S.W. Tong, G.P. Liu, Real-time simplified variable domain fuzzy control of PEM fuel cell flow systems, Eur. J. Control 14 (3) (2008) 223–233.
[9] J.N. Lygouras, P.N. Botsaris, J. Vourvoulakis, V. Kodogiannis, Fuzzy logic controller implementation for a solar air-conditioning system, Appl. Energy 84 (12) (2007) 1305–1318.
[10] U. Zuperl, F. Cus, M. Milfelner, Fuzzy control strategy for an adaptive force control in end-milling, J. Mater. Process. Technol. 164–165 (2005) 1472–1478.
[11] X.G. Duan, H.X. Li, H. Deng, Robustness of fuzzy PID controller due to its inherent saturation, J. Process Contr. 22 (2) (2012) 470–476.
[12] O. Karasakal, M. Guzelkaya, I. Eksin, Online tuning of fuzzy PID controllers via rule weighing based on normalized acceleration, Eng. Appl. Artif. Intell. 26 (1) (2013) 184–197.
[13] H. Boubertakh, M. Tadjine, P.Y. Glorennec, Tuning fuzzy PD and PI controllers using reinforcement learning, ISA Trans. 49 (4) (2010) 543–551.
[14] R.E. Precup, R.C. David, E.M. Petriu, M.-B. Rădac, S. Preitl, J. Fodor, Evolutionary optimization-based tuning of low-cost fuzzy controllers for servo systems, Knowl.-Based Syst. 38 (2013) 74–84.
[15] E. Sanchez, T. Shibata, L.A. Zadeh, Genetic Algorithms and Fuzzy Logic Systems, World Scientific, River Edge, NJ, 1997.
[16] J. Kennedy, R.C. Eberhart, Particle swarm optimization, in: Proceedings of the IEEE International Conference on Neural Networks, vol. 4, Perth, Australia, 1995, pp. 1942–1948.
[17] S.E. Mansour, G.C. Kember, R. Dubay, Online optimization of fuzzy-PID control of a thermal process, ISA Trans. 44 (2) (2005) 305–314.
[18] S.K. Oh, H.J. Jang, W. Pedrycz, Optimized fuzzy PD cascade controller: a comparative analysis and design, Simul. Model. Pract. Theory 19 (1) (2011) 181–195.
[19] M.J. Mahmoodabadi, M.B. Salahshoor Mottaghi, A. Mahmodinejad, Optimum design of fuzzy controllers for nonlinear systems using multi-objective particle swarm optimization, J. Vib. Control 22 (3) (2016) 769–783.
[20] M. Sahib, A novel optimal PID plus second order derivative controller for AVR system, Eng. Sci. Technol. Int. J. 18 (2015) 194–206.
[21] J. Yi, N. Yubazaki, K. Hirota, Stabilization control of ball and beam systems, in: IEEE/IFSA World Congress and 20th NAFIPS International Conference, Jul 25–Jul 28, vol. 4, Vancouver, BC, Canada, 2001, pp. 2229–2234.
[22] J. Yi, N. Yubazaki, Stabilization fuzzy control of inverted pendulum systems, Artif. Intell. Eng. 14 (2000) 153–163.